

Microstructure and mechanical properties of nickel deformed by hydrostatic extrusion

M. KULCZYK^{1,3*}, W. PACHLA¹, A. MAZUR¹, R. DIDUSZKO², H. GARBACZ³,
M. LEWANDOWSKA³, W. ŁOJKOWSKI¹, K. J. KURZYDŁOWSKI³

¹Institute of High Pressure Physics, Polish Academy of Sciences,
ul. Sokołowska 29/37, 01-142 Warsaw, Poland

²Institute of Electronic Materials Technology, ul. Wolczyńska 133, 01-919 Warsaw, Poland

³Warsaw University of Technology, Faculty of Materials Science and Engineering,
ul. Wołoska 141, 02-507 Warsaw, Poland

The goal of the present work is to demonstrate that a bulk, ultra-fine grained microstructure can be obtained by the hydrostatic extrusion process of a 99.5% technical purity of nickel. Deformation with the total true strain of 3.8 was performed at room temperature to a wire 3 mm in diameter. Microstructure was characterized by light microscopy, TEM, XRD and mechanical properties. Hydrostatic extrusion was shown to be an effective method of severe plastic deformation, which allows ultra-fine grained structures to be obtained within the deformed material. After cumulative hydrostatic extrusion, the yield stress tripled, reaching a maximum of 812 MPa with a moderate elongation of 13%. A mean subgrain size of 200 nm was observed, with a considerable diversity in the size of individual grains. For the final passes of hydrostatic extrusion, a slight decrease in the mechanical properties was observed, accompanied with an increase in crystallite size. This is explained in terms of thermal softening processes activated by the heat generated during hydrostatic extrusion.

Key words: *severe plastic deformation; hydrostatic extrusion; ultra-fine grains; nanocrystalline structure; grain refinement*

1. Introduction

Severe plastic deformation (SPD) is commonly applied to generate nanostructures in metals. By SPD methods the mean grain size is usually reduced to 100–500 nm (ultra-fine grained structures, UFG), and even below 100 nm (nanocrystalline structures, NC). This results in substantial strength increase, accompanied by a reduction

*Corresponding author, e-mail: mariusz@unipress.waw.pl

in toughness. In some cases, however, the SPD technique has allowed very promising combinations of high strength and ductility to be achieved [1, 2].

Up to now, the main SPD techniques having been studied for bulk metals are: high pressure torsion (HPT) [3, 4–6], equal-channel angular pressing (ECAP) [3, 7, 8], multiple rolling [9, 10], and cyclic extrusion-compression (CEC) [11]. The majority of the metals investigated by these methods were ductile metals, such as copper and aluminium and its alloys [2]. Somewhat harder materials, such as Fe [12], Ni [20], or Al–Ti [13] and Al–Fe–Ni [14] alloys, were usually processed by the powder consolidation of nanopowders. Powder methods, however, often result in low ductility of the final products [1]. Recently, the hydrostatic extrusion (HE) method has been used for obtaining NC structures in metals [15, 16]. The HE process has been used to generate NC structures in aluminium, aluminium alloys, and titanium [15, 16].

NC nickel has been processed into thin films by electro-deposition techniques [17, 18]. The development of an effective fabrication method that allows bulk, large volumes of NC nickel to be obtained may be an alternative for the consolidation of nanopowders [2, 3]. Only few literature data on ultra-fine grained UFG nickel, processed by HPT (grains ~ 100 nm) [19] and ECAP combined with rolling (grains ~ 300 nm) [3], have been reported up to now. On the other hand, nickel characterized by high strength and good ductility can find immediate application in micro-electro-mechanical systems (MEMS) [20–25].

In the present paper, the effect of cumulative HE on the microstructure and mechanical properties of nickel of 99.5% technical purity are presented and discussed.

2. Experimental

Nickel of technical purity 99.5% in the shape of a forged rod was used for machining the billet for hydrostatic extrusion in the form of a cylinder with $OD = 20$ mm and length 50 mm. Cumulative (multi-pass) HE was run in seven consecutive passes, with a total true strain 3.8, the strain rates varying between 2.3 s^{-1} and $1.18 \times 10^2 \text{ s}^{-1}$, and the extrusion pressure ranging between 500 MPa and 1400 MPa. The final diameter of the extruded wire was 3 mm. The macrostructure of the initial material and after the first three passes of HE was evaluated by light microscopy (METAVAL Zeiss). Specimen for light microscopy were polished and chemically etched with the solution containing HNO_3 (85 cm^3), HCOOH (18 cm^3), H_2O (17 cm^3). The microstructure of the final wire was investigated by transmission electron microscope (Philips EM-300), and the texture and crystallite size were investigated by X-ray diffraction using CuK_α radiation (Siemens D500). All structural investigations were made on the transverse cross sections of the extruded wires. The ultimate tensile strength, yield stress, and elongations were evaluated at room temperature from tensile (MTS-810) and compression (QTEST/10-MTS) tests under a $2 \times 10^{-3} \text{ s}^{-1}$ strain rate. Microhardness and microhardness distribution tests were also measured (Zwick-HV0.2/15).

3. Results and discussion

The initial material shows a mean grain size of $\sim 200\ \mu\text{m}$ (Fig. 1a), and the material contains annealing twins. The macrostructure after three passes of HE with the total strain $\varphi = 2.77$ is shown in Fig. 1b. Apparently, the macrostructure undergoes drastic refinement and shows substantial disturbance, confirming the large degree of deformation (almost 95% reduction).

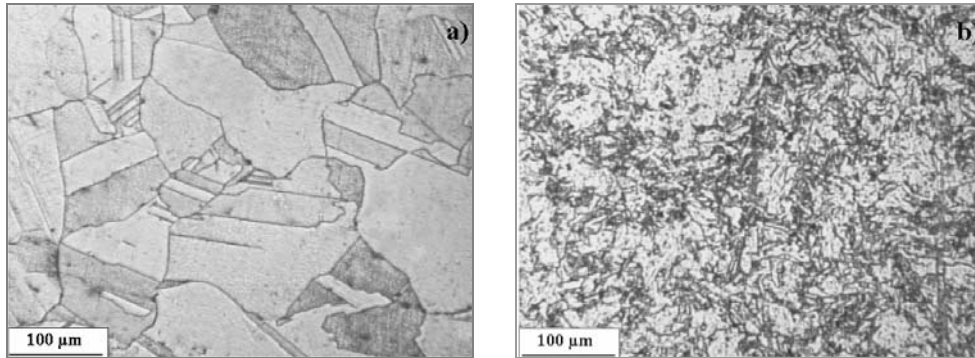


Fig. 1. Light microscopy images of nickel 99.5%:
a) the initial state (before HE), b) after three consecutive hydrostatic extrusion passes (true strain $\varphi = 2.77$)

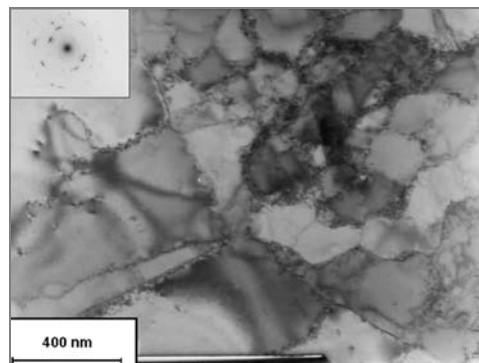


Fig. 2. TEM image of the microstructure of nickel 99.5% after seven consecutive hydrostatic extrusion passes (true strain $\varphi = 3.8$)

Figure 2 shows a TEM image of nickel after seven consecutive extrusion passes (true strain $\varphi = 3.8$). Subgrains with an approximate mean size $\sim 200\ \text{nm}$ are observed. The mean diameter of grains is reduced by ~ 1000 times, starting from $200\ \mu\text{m}$ down to ultra-fine subgrain structure. X-ray diffraction patterns have thereby revealed low misorientation angles between individual subgrains. The observed microstructure is non-uniform (inhomogeneous) and subgrain sizes vary substantially. For structural applications, it is even better to generate an inhomogeneous substructure, substantially differing in grain size [1]. As has been reported, such a mixed substructure leads

to the optimum combination between strength and ductility. Therefore, the highly inhomogeneous substructure obtained in the present work (Fig. 2) can be advantageous from the point of view of future applications. Up to now, such mixed structures have been obtained in copper [26, 27], with micrometer size grain content ~25 vol. %, and in zinc [28] and aluminium alloys [29]. According to previous investigations, nanograins are crucial for obtaining high strength and micrometer sized grains stabilize the plastic deformation process in metals [1, 26, 27].

To evaluate the ultra-fine grained structure behaviour within deformed nickel, XRD scans on the transverse cross sections of the extruded wires were made. Already after the first extrusion pass ($\varphi = 1.38$), the substantial refinement of crystallite domains in all selected crystallographic orientations was observed (Fig. 3). Further extrusion passes led to much smaller crystallite decrease, with an evident increase (approximately 30% in the $\langle 111 \rangle$ direction) in the last extrusion pass ($\varphi = 3.8$).

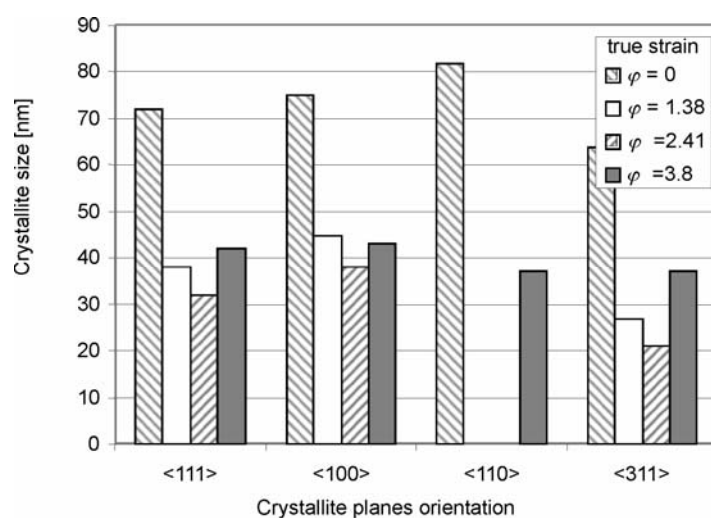


Fig. 3. Crystallite sizes in hydrostatically extruded nickel 99.5% for four crystallite planes orientations, evaluated from X-ray diffraction patterns

The texture in nickel after consecutive extrusion passes was also evaluated in a quantitative way. Table 1 shows the volume content of crystallites in a given orientation. In comparison to isotropic material, $\langle 110 \rangle$ crystallite orientation dominates in the initial state, which can be attributed to rod forging. After the first extrusion pass ($\varphi = 1.38$) a domination of $\langle 111 \rangle$ begins, which continues to increase with subsequent passes. This is a typical texture of the axis-symmetrical deformation processes of wire drawing [30]. After the fourth pass ($\varphi = 2.98$), the contribution of $\langle 111 \rangle$ crystallites starts to decrease and a new orientation, $\langle 311 \rangle$, emerges. This is accompanied by an increase in crystallite sizes, resulting from the result of heat generated during high-speed severe extrusion [31], which plays a more meaningful role for thinner wires during the last extrusion passes. Thin wires with a high surface-to-volume ratio

are more susceptible to recovery and recrystallization activated by temperature increase due to friction and the work of deformation. Microstructure recovery leads to a decrease in strength and an increase in the ductility of the material.

Table 1. Volume content of coherent domains in nickel 99.5% after consecutive hydrostatic extrusion passes

Crystallo-graphic direction	Isotropic Ni	Initial material	Number of extrusion passes					
			1 ($\varphi^1 = 1.38$)	2 ($\varphi = 2.41$)	3 ($\varphi = 2.77$)	4 ($\varphi = 2.98$)	5 ($\varphi = 3.21$)	7 ($\varphi = 3.8$)
<111>	0.16	0.156	0.863	0.803	0.819	0.782	0.743	0.701
<200>	0.12	0.083	0.064	0.142	0.116	0.107	0.100	0.067
<220>	0.24	0.285	0.000	0.005	0.004	0.009	0.011	0.016
<311>	0.48	0.477	0.074	0.051	0.062	0.103	0.147	0.216

¹ φ – true strain.

Microhardness measurements have confirmed the recovery processes (Fig. 4). A maximum microhardness of 2.27 GPa has been measured after the fourth pass with $\varphi = 2.98$, (an increase of 1.7 times compared to the initial material). The yield stress also reaches a maximum for a true strain of $\varphi = 2.98$. At this stage, the yield stress has tripled, reaching 812 MPa. Although the largest increase in microhardness and strength was measured after the first extrusion pass ($\varphi = 1.38$), it is attributed to the highest reduction applied for that pass. The final yield stress (after 7 extrusion passes, $\varphi = 3.8$) reached 783 MPa, i.e. 2.8 times larger than for the initial material. The respective increase in ultimate tensile strength was 2.5. This was accompanied by a drop in elongation of 40–13%.

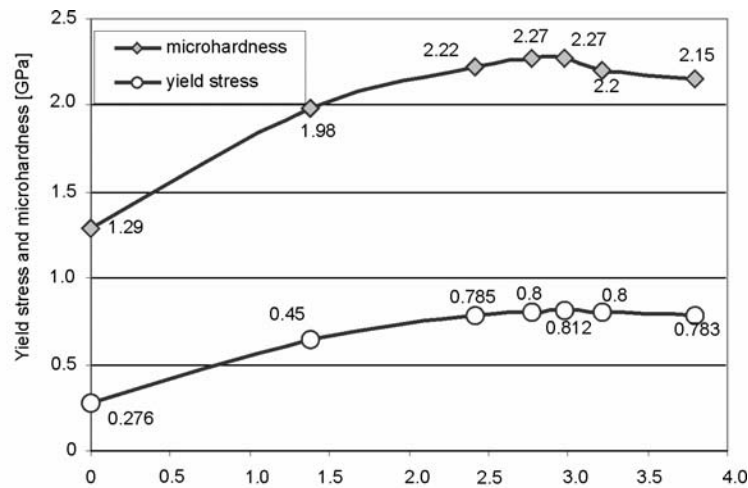


Fig. 4. Microhardness (HV0.2) and yield stress of nickel 99.5% after consecutive hydrostatic extrusion passes

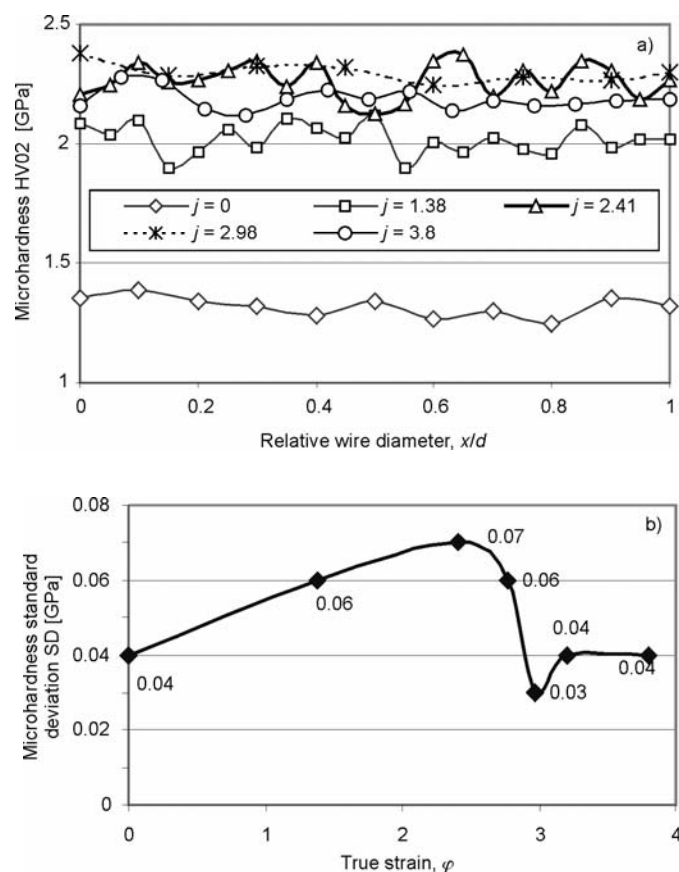


Fig. 5. Microhardness distribution at the transverse cross sections of nickel 99.5% wires (a), and the standard deviation (SD) of microhardness plotted against the true strain in hydrostatic extrusion (b)

The transformations of the microstructures in extruded nickel are well seen on the microhardness distribution graphs measured across the extruded wires (Fig. 5a). The initial, relatively stable distribution of microhardness shows higher oscillations in the intermediate range of extrusions, and recovers its high uniformity for the fourth pass ($\phi = 2.98$) of the extrusion. With further deformation, disordering begins again and progressively increases up to the seventh pass ($\phi = 3.8$). The standard deviations, SD , of microhardness are plotted as functions of true strain in Figure 5(b). The initial material is characterized by lower variations in microhardness, confirming its homogeneity. With an increasing number of HE passes, homogeneity decreases (SD increases), and at a certain true strain suddenly drops. After the fourth pass, $\phi = 2.98$ (wire diameter 4.5 mm), SD is lowest, which suggests a highest homogeneity of microstructure. Further passes result in an increase of SD , indicating that the microstructure changes (homogeneity decreases again).

Table 2. Comparison between the mechanical properties of nickel after ECAP, rolling, and annealing [3] and nickel after cumulative hydrostatic extrusion (present work)

Material history	Ultimate tensile strength, UTS [MPa]	Yield stress 0.2% YS [MPa]	Elongation to fracture ε [%]
8 passes of ECAP ¹ + cold rolling + annealing 200 °C/1h	890	835	11.7
7 passes of hydrostatic extrusion	820	783	13.0

¹ECAP – equal channel angular pressing.

In Ref. [3], an ultra-fine grained microstructure in nickel has been generated by the combination of two methods, ECAP and rolling, followed by final heat treatment. In Table 2, the results of the complex, thermomechanical procedure of Ref. [3] are compared with the results of the present research, in which the HE process alone (without final heat treatment) has allowed similar mechanical properties to be achieved with the same level of elongation.

4. Conclusions

Nickel of 99.5% purity has been hydrostatically extruded with a cumulative strain of 3.8. Remarkable microstructure refinement by three orders of magnitude (initial grains of 200 μm to final subgrains of 200 nm) was observed. The transformation in microstructure was accompanied by a substantial increase in mechanical properties (~ 3 times in yield stress and over 1.7 times in microhardness). After the final passes of extrusion, a coarsening of the microstructure was observed, accompanied by a decrease in yield stress and microhardness. This can be attributed to the recovery processes activated by thermal effects generated during high speed ($\sim 1.2 \times 10^2 \text{ s}^{-1}$) hydrostatic extrusion. Moderate ductility ($\varepsilon \sim 13\%$) in extruded wires can be attributed to the mixed (non-uniform) character of the microstructure obtained after extrusion (a wide variety in subgrain sizes and defect content). Using cumulative hydrostatic extrusion, 99.5% nickel with high strength (above 0.8 GPa), high hardness (above 3 GPa), and moderate ductility (13%) has been obtained, which brings closer the potential application of this material in, for example, MEMS systems.

Acknowledgements

Authors thank Mr. K. Wojciechowski from Institute of High Pressure Physics, Polish Academy of Sciences, for his assistance in performing hydrostatic extrusion tests.

References

- [1] VALIEV R., *Nature*, 3 (2004), 511.
- [2] VALIEV R.Z., ISLAMGALIEV R.K., ALEXANDROV I.V., *Progr. Mater. Sci.*, 45 (2000), 103.

- [3] KRASILNIKOV N., ŁOJKOWSKI W., PAKIEŁA Z., VALIEV R., Solid State Phenomena, 94 (2003), 51.
- [4] IVANISENKO YU., VALIEV R.Z., FECHT H.-J., Mater. Sci. Eng. A, 390 (2005), 159.
- [5] ZHILYAEV A.P., NURISLAMOVA G.V., KIM B.-K., BARO M.D., SZPUNAR J.A., LANGDON T.G., Acta Mater., 51 (2003), 753.
- [6] JIANG H., ZHU Y.T., BUTT D.P., ALEXANDROV I.V., LOWE T.C., Mater. Sci. Eng., A290 (2000), 128.
- [7] STOLYAROV V.V., ZHU Y.T., LOWE T.C., VALIEV R.Z., Mater. Sci. Eng., A303 (2001), 82.
- [8] STOLYAROV V.V., LAPOVOK R., BRODOVA I.G., THOMSON P.F., Mater. Sci. Eng., A357 (2003), 159.
- [9] GIGUERE A., HAI N.H., DEMPSEY N., GIVORD D., J. Magn. Magn. Mater., 242–245 (2002), 581.
- [10] SAGEL A., SIEBER H., FECHT H. J., PEREPEZKO J. H., Phil. Mag. Lett., 77 (1998), 109.
- [11] RICHERT M., LIU Q., HANSEN N., Mater. Sci. Eng., A260 (1999), 275.
- [12] TAKAKI S., KAWASAKI K., KIURA Y., J. Mater. Process. Technol., 117 (2001), 359.
- [13] GUOXIAN L., ZHIMIN L., ERDE W., J. Mater. Process. Technol., 55 (1995), 37.
- [14] GUOXIAN L., MENG Q., LI Z., WANG E., Nanostructured Materials, 5 (1995), 673.
- [15] LEWANDOWSKA M., GARBACZ H., PACHLA W., MAZUR A., KURZYDŁOWSKI K.J., Solid State Phenomena, 101–102 (2005), 65.
- [16] LEWANDOWSKA M., GARBACZ H., PACHLA W., MAZUR A., KURZYDŁOWSKI K. J., Mater. Sci.-Poland, 23 (2005), 279.
- [17] WANG N., WANG Z., AUST K., ERB U., Mater. Sci. Eng., A237 (1997), 150.
- [18] XIAO C., MIRSHAMS R.A., WHANG S.H., YIN W.M., Mater. Sci. Eng., A301 (2001), 35.
- [19] KORZNIKOW V., PAKIEŁA Z., KURZYDŁOWSKI K.J., Acta Phys. Polon. A, 102 (2002), 265.
- [20] VALIEV R.Z., MISHRAL R.S., GROZAL J., MUKHERJEE A.K., Scripta Mater., 34 (1996), 1443.
- [21] HEMKER K.J., LAST H., Mater. Sci. Eng., A319–321 (2001), 882.
- [22] BUCHHEIN T.E., LAVAN D.A., MICHAEL J.R., CHRISTENSON T.R., LEITH S.D., Metall. Mat. Trans., A, 32A (2002), 539.
- [23] ROBERTSON A., ERB U., PALOMBO G., Nanostruct. Mater., 12 (1999), 1035.
- [24] YOUNG D.J., MRS Bulletin, April (2001), 331.
- [25] DE BOER M.P., MAYER T.M., MRS Bulletin, April (2001), 302.
- [26] WANG Y., CHEN M., ZHOU F., MA E., Nature, 419 (2002), 912.
- [27] MUGHRABI H., HÖPPEL H.W., KAUTZ M., VALIEV R.Z., Z. Metallkunde, 94 (2003), 1079.
- [28] ZHANG X., WANG H., SCATTERGOOX R.O., NARAYAN I., KOCH C.C., SERGUEEVA A.V., MUKHERJEE A.K., Acta Mater., 50 (2002), 4823.
- [29] PARK Y.S., CHUNG K.H., KIM N.J., LAVERNIA E.J., Mater. Sci. Eng., A374 (2004), 211.
- [30] COULOMB P., *Les textures dans les métaux de réseau cubique*, Dunod, Paris, 1972 (Polish translation: *Tekstura w metalach o sieci regularnej*, PWN, Warszawa, 1977).
- [31] WIŚNIEWSKI T.S., PACHLA W., KUKLA D., MAZUR A., KURZYDŁOWSKI K.J.K., QIRT 2004, 7th Int. Conf. on Quantitative Infrared Thermography, Rhode-St-Genèse, Belgium, July 5–8, 2004.

Received 22 March 2005